Hydraulic Erosion of Concrete by a Submerged Jet

H. Hocheng and C.H. Weng

(Submitted 21 November 2001)

The hydraulic erosion of concrete is often found in civil and marine engineering construction. The present study explores the effects of several erosion parameters on the material loss of a concrete specimen subject to the hydraulic flow produced by a submerged jet. Such an investigation has rarely been reported in the literature. The concrete specimen has a typical compressive strength of 35 MPa, and the experimental parameters include the exposure time, incidence angle, standoff distance, and the hydraulic jet pressure. The impinging velocity is estimated based on the distance considered in the round jet model. The regression analysis shows the relationship between each parameter and the material loss. One finds that the material loss is proportional to the exposure time and the hydraulic pressure. The maximum erosion lies at an incidence angle of around 30° to 45° and is affected by the fourth-order polynomial of impinging velocity. The result of the present study provides a reference to engineering practice where concrete erosion is a concern.

Keywords concrete, hydraulic erosion, impinging angle, standoff, water jet

1. Introduction

Concrete is widely applied in civil and marine construction. In the past, the principal development of concrete technology was to increase the compressive strength of concrete materials. As techniques for the production of concrete have became more sophisticated, the concrete industry has begun to consider the importance of durability as a concern that will overtake the importance of compressive strength in the future. From the viewpoint of material wear, durability indicates erosion resistance.[1]

When concrete is used in civil or marine construction, the most significant erosion problems are due to the attack of fast-flowing water over its surface.[2] Hydraulic erosion can be subdivided into the following three categories: (1) the kinetic erosion by the high-velocity water flow; (2) cavitation erosion; and (3) chemical corrosion. These erosions often show mutual interactions. For example, as the surface destruction of concrete is caused by the kinetic action of the high-velocity water flow or by cavitation erosion, aggressive chemicals become more effective in eroding concrete.

The current experimental study has focused on the kinetic and cavitation effects induced by the high-velocity flow, where the impinging velocity and exposure time are the most major parameters. There is a threshold value for the impinging velocity below which no erosion phenomenon can be observed, while a crack on the concrete surface can be found.[3] Since the impinging velocity is generated by the hydraulic pressure, it must exceed a critical pressure for hydraulic erosion to occur. This critical pressure is about 30 times the tensile strength of the concrete specimen.[4]

H. Hocheng and **C.H. Weng,** Department of Power Mechanical Engineering, National Tsing Hua University, Hsinchu, Taiwan, Republic of China. Contact e-mail: hocheng@pme.nthu.edu.tw.

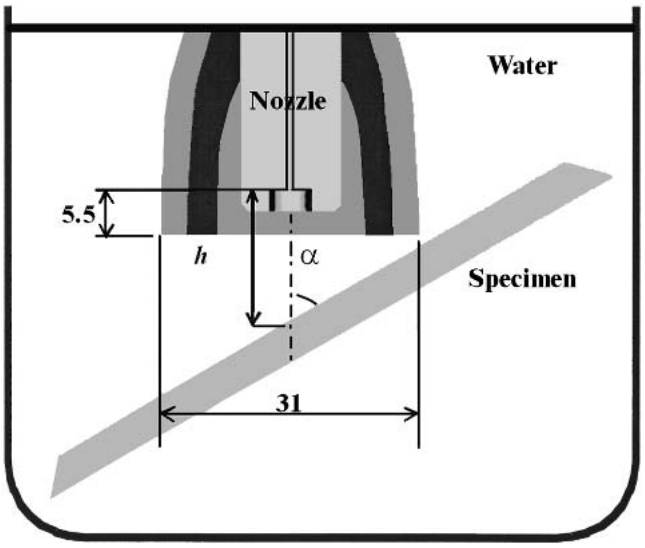

Fig. 1 Sketch of the experimental set-up

In the literature, the hydraulic erosion of concrete is investigated with the parameters of impinging velocity and exposure time, while the incidence angle and the standoff distance between nozzle exit and the specimen have not been considered. The angle of attack is of fundamental importance in predicting the hydraulic erosion of a concrete construction in an engineering application. The standoff distance determines the impinging velocity associated with the hydraulic pressure. These aspects have not been considered in other reports in the literature. A model is constructed in this study to correlate the hydraulic pressure, the standoff distance, and the resulting impinging velocity.

2. Experiment

2.1 Experimental Set-up

The sketch of the experimental set-up is shown in Fig. 1. The water jet is pressurized to impinge on the concrete speci-

men held by the fixture in a submerged environment. This fixture is made to be able to vary the standoff distance and the incidence angle. A stopwatch measures the exposure time. The impinging velocity can be estimated by the hydraulic pressure and the standoff distance. The detailed design of all parameters is listed in Table 1. In fact, the incidence angle affects the standoff distance as well as the impinging velocity, as can be seen in Fig. 1. Their true values are listed in Tables 2 and 3. In this study, the cavitation number was found to be >0.2; hence the effect of cavitation erosion can be neglected.[5,6] In other words, kinetic erosion is the major mechanism of concrete wear in this study. Besides, the fresh water environment causes little concern for chemical corrosion.

2.2 Experimental Material and Procedure

The specimen material is concrete of a typical compressive strength of 35 MPa. Its dimensions are $8 \times 8 \times 6$ cm^3, and each weighs 850 g. When immersed in water, concrete can absorb water and increase its weight from 2% to 5%. Because of the potential for moistening, the specimen follows a preset baking procedure to keep the moisture constant for a reliable measurement of the material loss. The specimen was placed in a baking oven for 30 min, then was sent to a thermostat container. The specimen weight was recorded day by day until the value became steady.

Table 1 Experimental Parameters

Parameters	Values
Exposure time (t)	10/20 min
Incidence angle (α)	90°/75°/60°/45°/30°/15°
Standoff distance (h)	Please consult Table 2
Hydraulic pressure (P)	70/140 Bar
Impinging velocity	Please consult Table 3

3. Impinging Velocity of a Round Jet

The following analysis was conducted to estimate the impinging velocity on the specimen in the current study. A turbulence jet can be divided into the following three regions: potential core flow; developing flow; and self-preserving flow (as shown in Fig. 2). In the potential core region, the maximum

Table 2 Standoff Distance

Incidence Angle	Standoff Distance (mm)
90°	10.0, 17.5, 25.0, 40.0
75°	17.2, 24.7, 32.2, 47.2
60°	22.0, 29.5, 37.0, 52.0
45°	28.5, 36.0, 43.5, 58.5
30°	39.9, 47.4, 54.85, 69.9
15°	70.9, 78.4, 85.9, 100.9

Table 3 Impinging Velocity (D = 1.2 mm)

Hydraulic Pressure	Incidence Angle	Impinging Velocity (m/s)
70 bar	90°	50.8, 43.7, 39.3, 31.0
70 bar	75°	46.3, 41.1, 34.3, 27.8
70 bar	60°	42.7, 37.4, 27.8, 24.8
70 bar	45°	38.7, 30.6, 25.3, 21.6
70 bar	30°	27.6, 23.3, 18.7, 17.7
70 bar	15°	15.6, 14.9, 12.8, 11.8
140 bar	90°	78.2, 64.9, 56.1, 35.1
140 bar	75°	65.4, 56.9, 43.6, 35.4
140 bar	60°	60.2, 47.6, 38.0, 27.0
140 bar	45°	49.2, 39.0, 32.2, 27.5
140 bar	30°	35.2, 29.6, 25.6, 20.1
140 bar	15°	19.8, 17.9, 16.3, 15.0

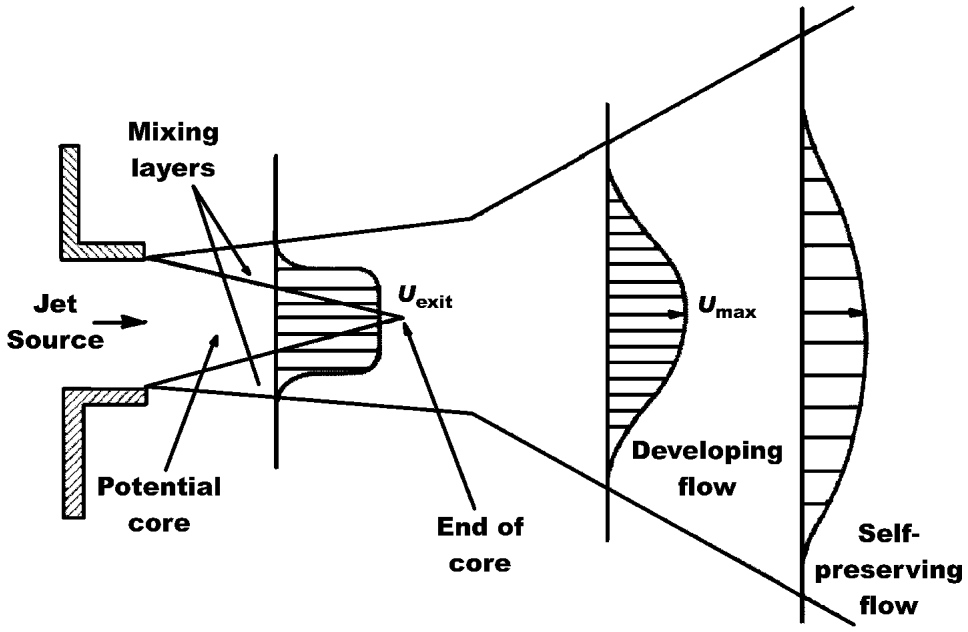

Fig. 2 The development of jet flow

flow velocity is equal to the exit jet velocity. The potential core decayed quickly, at a distance of about one initial diameter from the jet exit. The velocity profile in the developing flow region was approximately Gaussian. At about 20 times the initial diameters downstream from the exit, the velocity profile stabilized and maintained the self-preserving region, as a function of the redial distance from the centerline only.[7]

One assumes the constant momentum of the round jet as

$$J = \rho \int_{-\infty}^{+\infty} u^2 dy = \text{const} \qquad \text{(Eq 1)}$$

where u is the velocity in the jet direction, ρ is the density of flow, and y is the radial coordinate. In the region of the developing flow, the velocity profile is[7]

$$\frac{\overline{u}}{U_{\max}} = s\, h^2 \left[0.2752 \left(\frac{J\rho}{\mu^2 x^2} \right)^{1/3} y \right] \qquad \text{(Eq 2)}$$

where $\overline{u}$ is the mean velocity, $U_{\max}$ is the maximum velocity on the centerline, μ is the viscosity of water, and x is the distance coordinate from the jet exit.[8] In the self-preserving flow region of a round jet, the velocity profile varying with the jet radius is[9]

$$\frac{\overline{u}}{U_{\max}} = s\, h^2 \left[10.4 \left(\frac{y}{x^2} \right) \right] \qquad \text{(Eq 3)}$$

Based on Fig. 1, the nozzle exiting velocity can be determined to be 158.6 m/s under the conditions of a nozzle diameter (D) of 1.2 mm, a density of 1000 kg/m^3, and a viscosity of 0.89 MPa. Substituting those data into Eq 1, one can estimate the jet momentum to be 213.16 kg/m^2/s^2 at the nozzle exit. As the momentum is substituted into Eq 2 and 3, the maximum flow velocity on the centerline can be determined.

The following assumptions are made for practical purposes. First, the transitions between the potential core and the developing flow, and between the developing flow and the self-preserving flow occur at a distance of 1 and 20 times the nozzle diameter, respectively. Second, the jet width is equal to one diameter as it exits the potential core, and this satisfies Eq 4 at a distance of 20 times the diameter. The jet width of the developing flow increases linearly from the beginning to the end. By using these equations and assumptions, the maximum centerline velocity and the jet width can be calculated. The results are shown in Fig. 3 and 4, and in Table 4. Based on these results, the effects of impinging velocity on hydraulic erosion can be discussed.

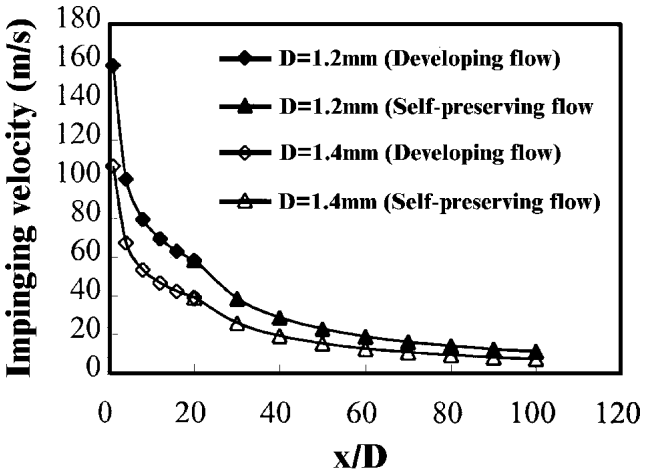

Fig. 3 The decay of the impinging velocity

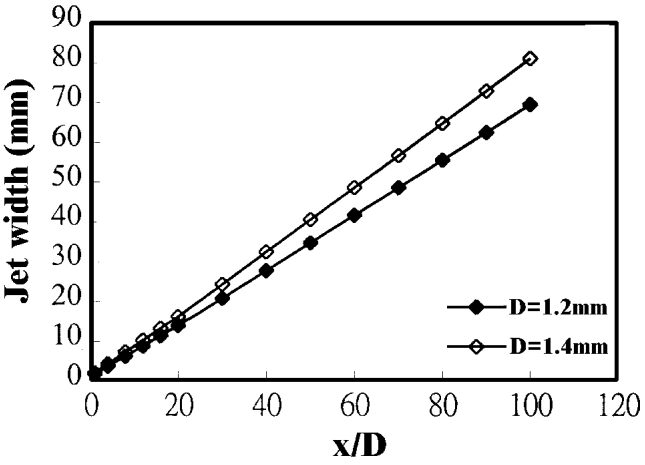

Fig. 4 The development of the jet width

Table 4 Maximum Centerline Velocity and Jet Width

Nozzle Diameter (mm)	Standoff Distance (mm)	Maximum Centerline Velocity (m/s)	Jet Width (mm)
1.2	$1.2 \le h \le 4$	$U_{\max} = 168.53h^{-1/3}$	$b = 1.2 + 0.53h$
	$h \ge 24$	$U_{\max} = 1402.62h^{-1}$	$b = 0.58h$
1.4	$1.4 \le h \le 28$	$U_{\max} = 119.47h^{-1/3}$	$b = 1.4 + 0.53h$
	$h \ge 28$	$U_{\max} = 1083.63h^{-1}$	$b = 0.58h$

4. Experimental Results and Discussion

4.1 Effects of Exposure Time

The relationship of exposure time and material loss at various incidence angles is shown in Fig. 5. The material loss of concrete is nearly proportional to exposure time. It shows that the hydraulic erosion is quite stable and that the accumulated result of the material loss is on a small scale. One also notes that the erosion effect is most evident at an incidence angle of 30° to 45°. This fact will be illustrated and discussed more extensively in the next section.

4.2 Effects of Incidence Angle

The second parameter is the incidence angle with covariances of exposure time and standoff distance. Figure 6 illustrates the relationship between the incidence angle and the material loss. The maximum value of material loss is found at an incidence angle of around 30° to 45°. As the incidence angle

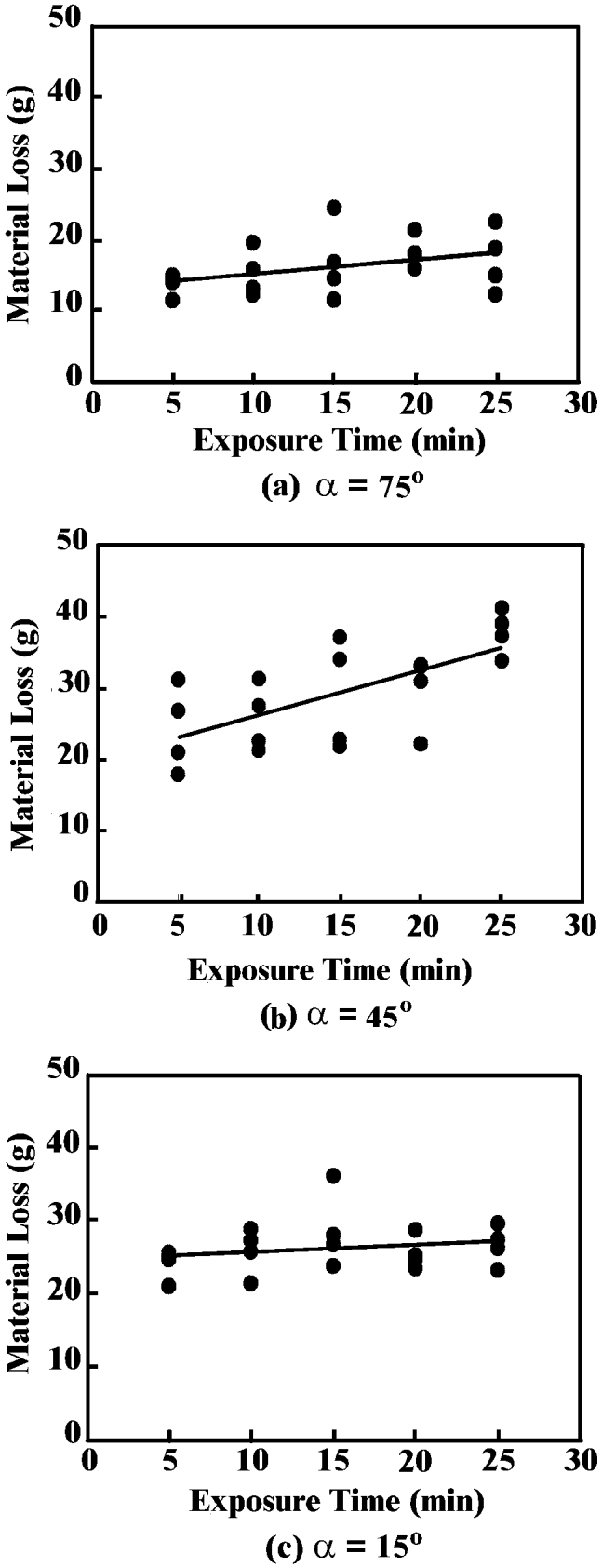

Fig. 5 Correlation between exposure time and material loss (140 bar): **(a)** 75; **(b)** 45; and **(c)** 15

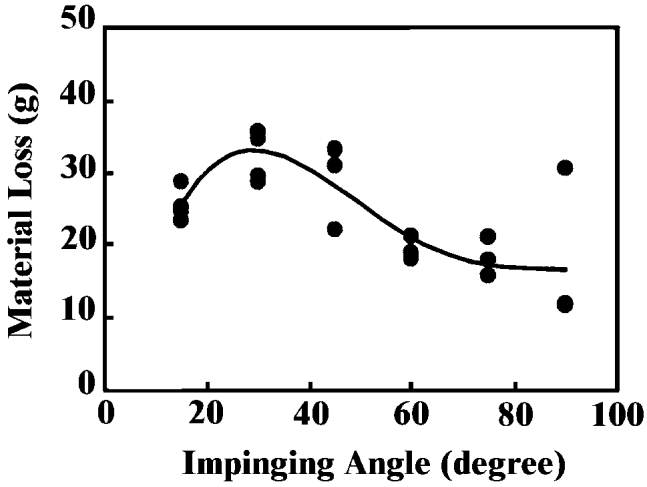

Fig. 6 Correlation between the impinging angle and material loss (140 bar, 20 min)

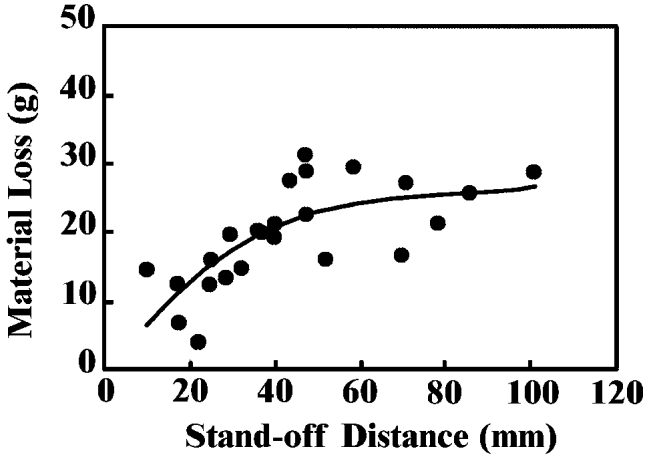

Fig. 7 Correlation between standoff and material loss (140 bar, 20 min)

increases, the area of jet flow increases. On the other hand, the cutting erosion is enhanced as the incidence angle decreases. Since the material loss is the product of the erosion area and the erosion per unit area, the material loss has a maximum value at around 30-45° of the impinging angle.

4.3 Effects of Standoff Distance

Figure 7 shows the correlation between the standoff distance and the material loss. The material loss increases with the jet width as the jet develops at a lower standoff distance, while it saturates as the impinging velocity decays at a large standoff distance. As shown in Table 4, the impinging velocity decays more significantly at a large standoff distance, say, 30 mm, while the impinging area (depicted by the jet width) increases accordingly. Therefore, the material loss influenced by both terms is saturated at large standoff distance.

4.4 Effects of Impinging Velocity

Figure 8 shows the effect of impinging velocity. The material loss increases with the impinging velocity by a power of

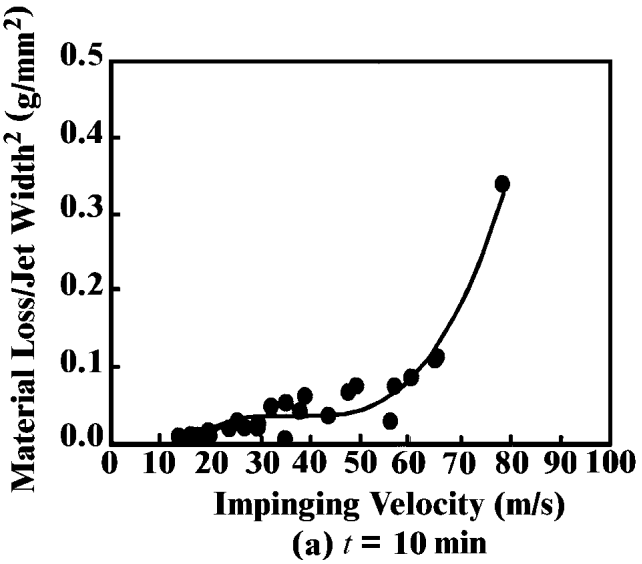

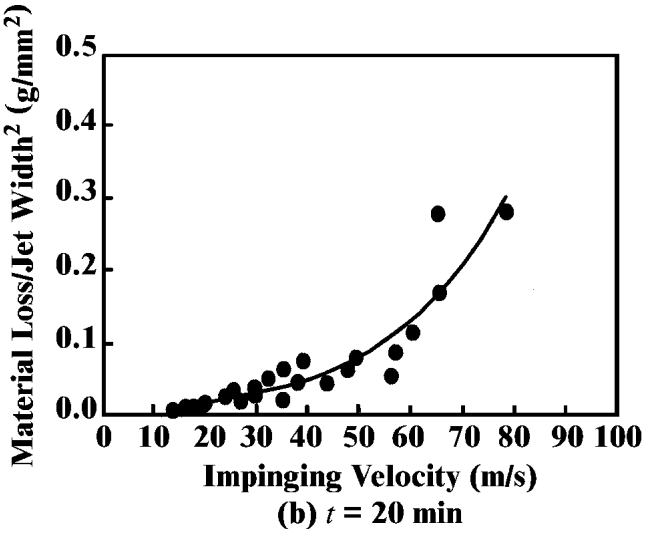

Fig. 8 Correlation between the impinging velocity and material loss (140 bar): **(a)** t = 10 min; and **(b)** t = 20 min

four. Since the jet flow width is inversely proportional to the impinging velocity, the material loss per unit of area in fact increases with the square of the impinging velocity.

4.5 Effects of Hydraulic Pressure

Figure 9 shows that higher hydraulic pressure produces more erosion of the material. This is attributed to the increased exit velocity from the nozzle, as Fig. 10 shows.

5. Conclusions

The hydraulic erosion of concrete by a submerged jet flow was investigated in this study. In addition to the effects of impinging velocity and exposure time, the incidence angle and standoff distance were found to be very influential on erosion.

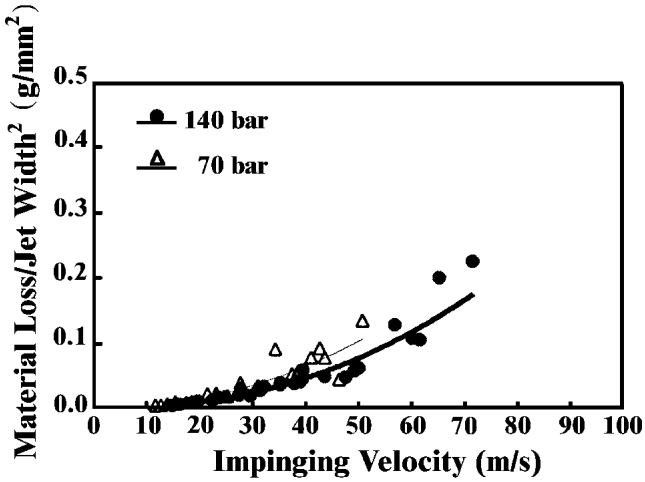

Fig. 9 Effect of hydraulic pressure on material loss (20 min)

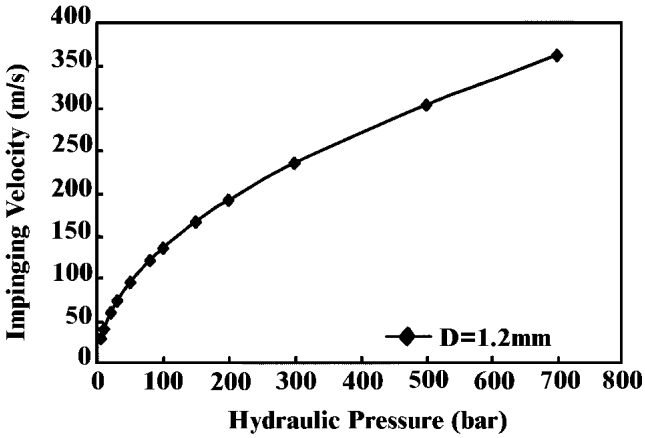

Fig. 10 Correlation between hydraulic pressure and nozzle exit velocity

The effect of the latter was elaborated on by the analysis of the impinging velocity and the jet width varying with the standoff distance. This analysis is based on the model of a round jet, which shows the development and transition of the jet downstream. The following conclusions can be made:

- The material loss is proportional to the exposure time.
- The maximum material loss occurs at an incidence angle of around 30-45°.
- The effect of the standoff distance on material loss is shown implicitly by the influence of both the impinging velocity and the jet width.
- The material loss is proportional to the cross-sectional area of jet flow, namely, the square of the jet width.
- The jet width of jet flow is inversely proportional to the impinging velocity, while the material loss varies with the second-order polynomial of impinging velocity.

References

1. P.C. Aitcin: "Cements of Yesterday and Today, Concrete of Tomorrow," *Cement Concrete Res.*, 2000, *30*, pp. 1349-59.

2. A.P. Davis: "Safe Velocity of Water on Concrete," *Eng. News*, 1912, pp. 1-20.
3. A.W. Momber and R. Kovacevic: "Fundamental Investigations on Concrete Wear by High Velocity Water Flow," *Wear*, 1994, *177*, pp. 55-62.
4. H.J. Powell and S.P. Simpson: "Theoretical Study of Mechanical Effects of Water Jets Impinging on Semi-Infinite Elastic Solid," *Int. J. Rock Mech. Mining Sci.*, 1969, *6*, pp. 353-64.
5. H. Hocheng and M.Y. Hsu: "Erosion Wear of Stainless Steel by Abrasives Entrained in a Water Jet," *Arabian J. Sci. Eng.*, 2000, *25*, pp. 187-202.
6. K.H. Frizell and B.W. Mefford: "Designing Spillways to Prevent Cavitation Damage," *Concrete Int.*, 1991, pp. 58-64.
7. F.M. White: *Viscous Fluid Flow*, 2nd ed., McGraw-Hill, New York, NY, 1991, pp. 470-76.
8. H. Schlichting and Z. Angew: "Laminare Strahlenausbreitung," *Math. Mech.*, 1933, *13*, pp. 260-63.
9. I. Wygnanski and H.J. Fiedler: "Some Measurements in the Self-Preserving Jet," *Fluid Mech.*, 1969, *38*, pp. 577-612.